Supplement of Atmos. Meas. Tech., 18, 5087–5101, 2025
https://doi.org/10.5194/amt-18-5087-2025-supplement

Atmospheric Measurement Techniques
Open Access
EGU

Supplement of

Characterization of the newly designed wall-free particle evaporator (WALL-E) for online measurements of atmospheric particles

Linyu Gao et al.

Correspondence to: Matthieu Riva (matthieu.riva@ircelyon.univ-lyon1.fr)

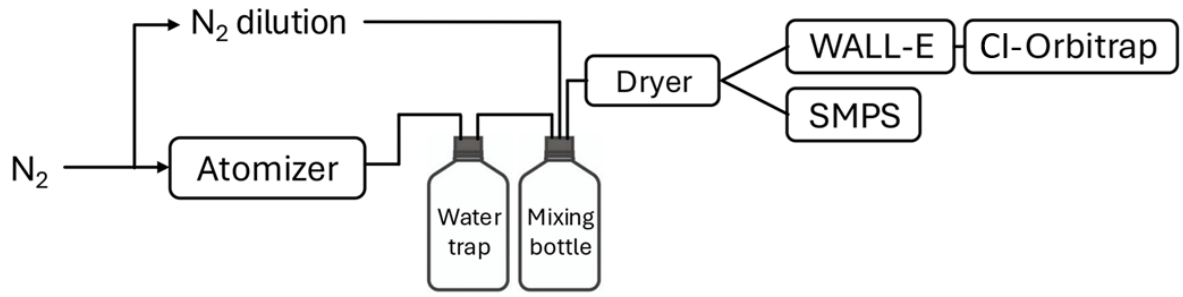

Figure S1. Experimental setup for the atomisation of standard solutions.

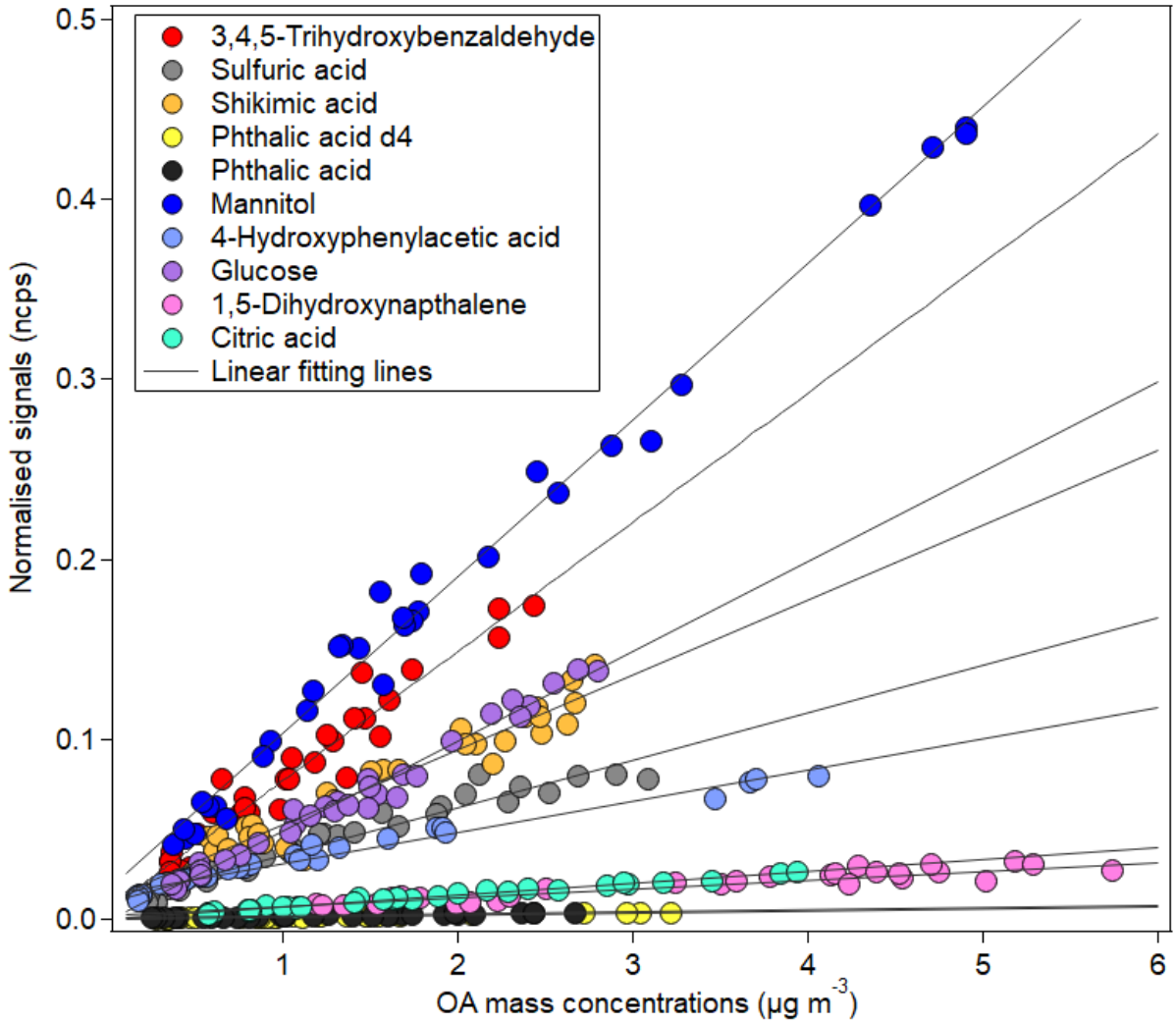

Figure S2. Wall-E CIMS response for each standard, compared with OA mass concentrations measured with an SMPS.

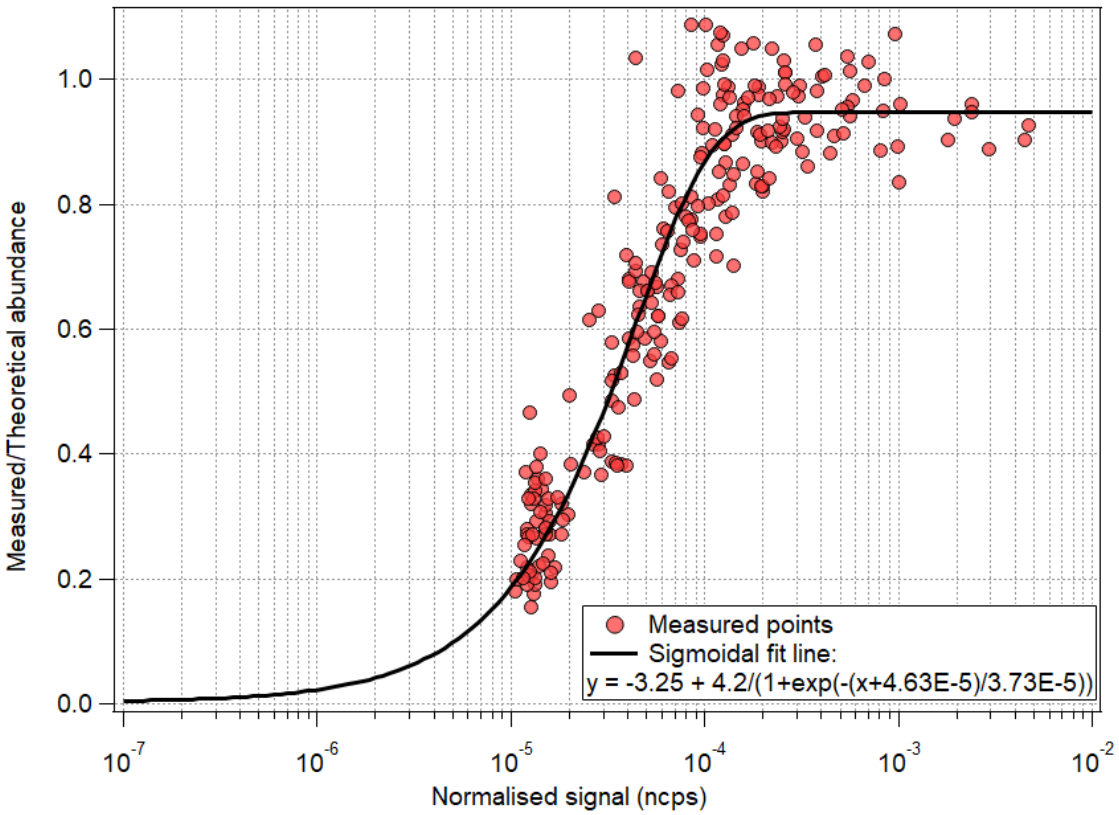

Figure S3. Linearity correction on Orbitrap data. Data is fitted by a sigmoidal function.

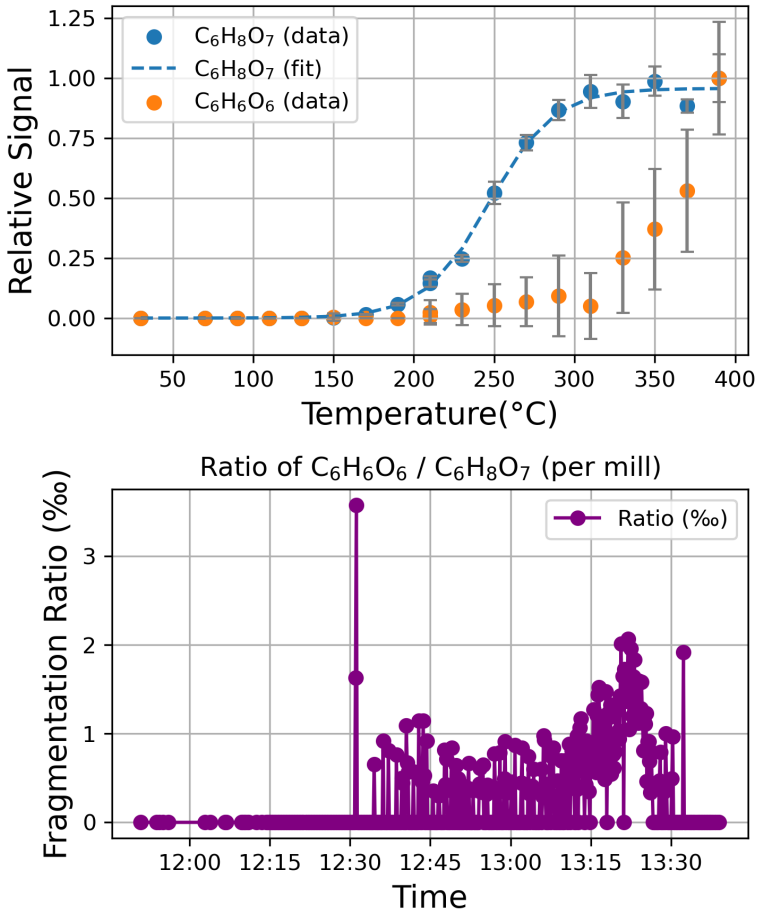

Figure S4. Upper plot shows the Citric Acid ($C_6H_8O_7$) thermogram in Blue, along with citric acid fragments in Orange ($C_6H_6O_6$), plotted as a relative signal. Lower plot presents the fragmentation ratio per mille under different conditions.

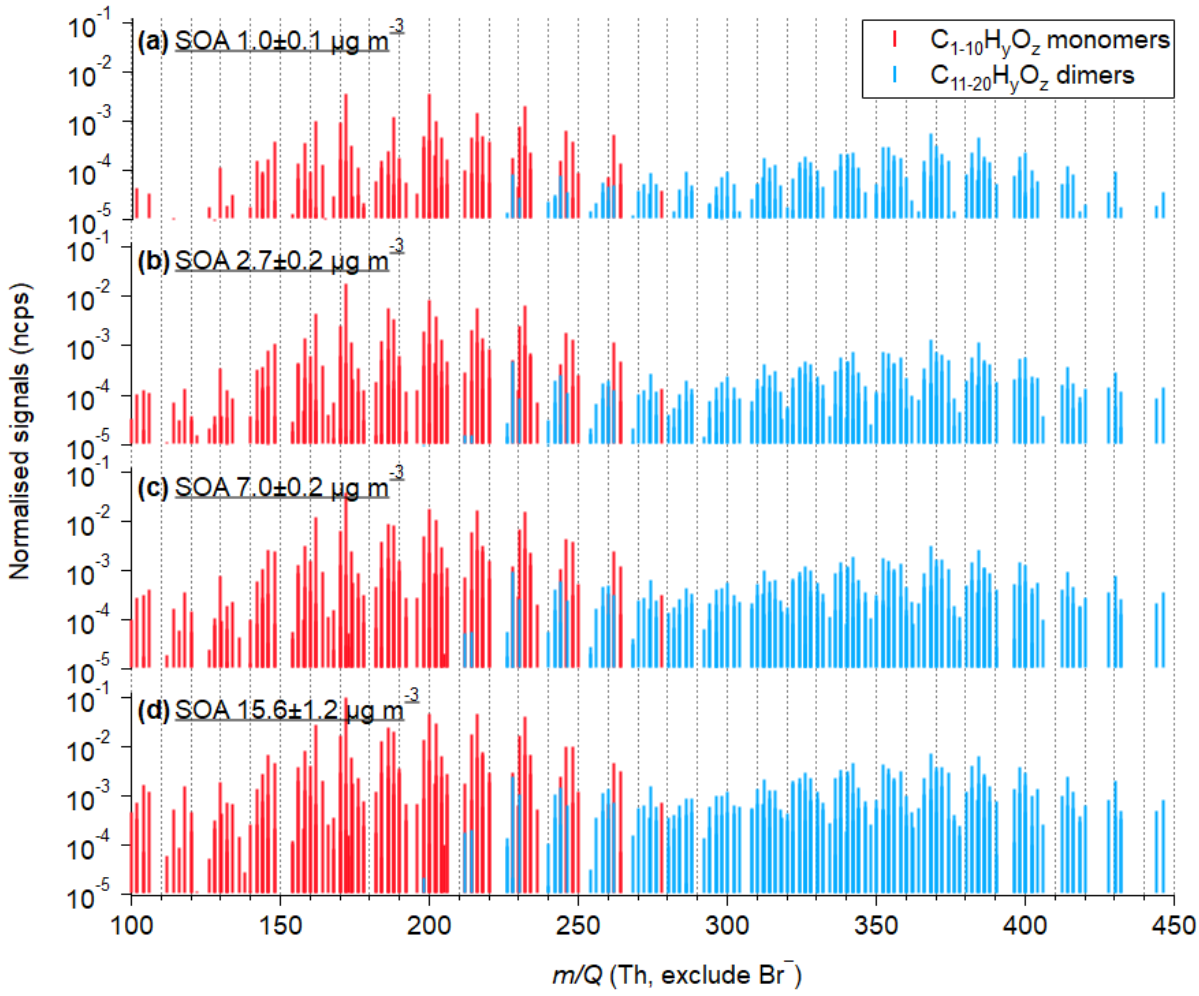

Figure S5. Logarithmic Mass spectra of particle-phase organic compounds formed from the oxidation of α-pinene under varying mass particle concentrations (1.0-15.6 μg m^{-3}). Compounds are evaporated and detected by the WALL-E CIMS with hot sheath flow and TD temperatures of 300 ºC, sampling flow of 1 SLPM, hot dilution flow of 0.25 SLPM, and a cold dilution flow of 10 SLPM. Signals are normalized to Br– signal intensity. Red and blue refer to monomers ($C_{1\text{-}10}H_yO_x$) and dimers ($C_{11\text{-}20}H_yO_x$), respectively.

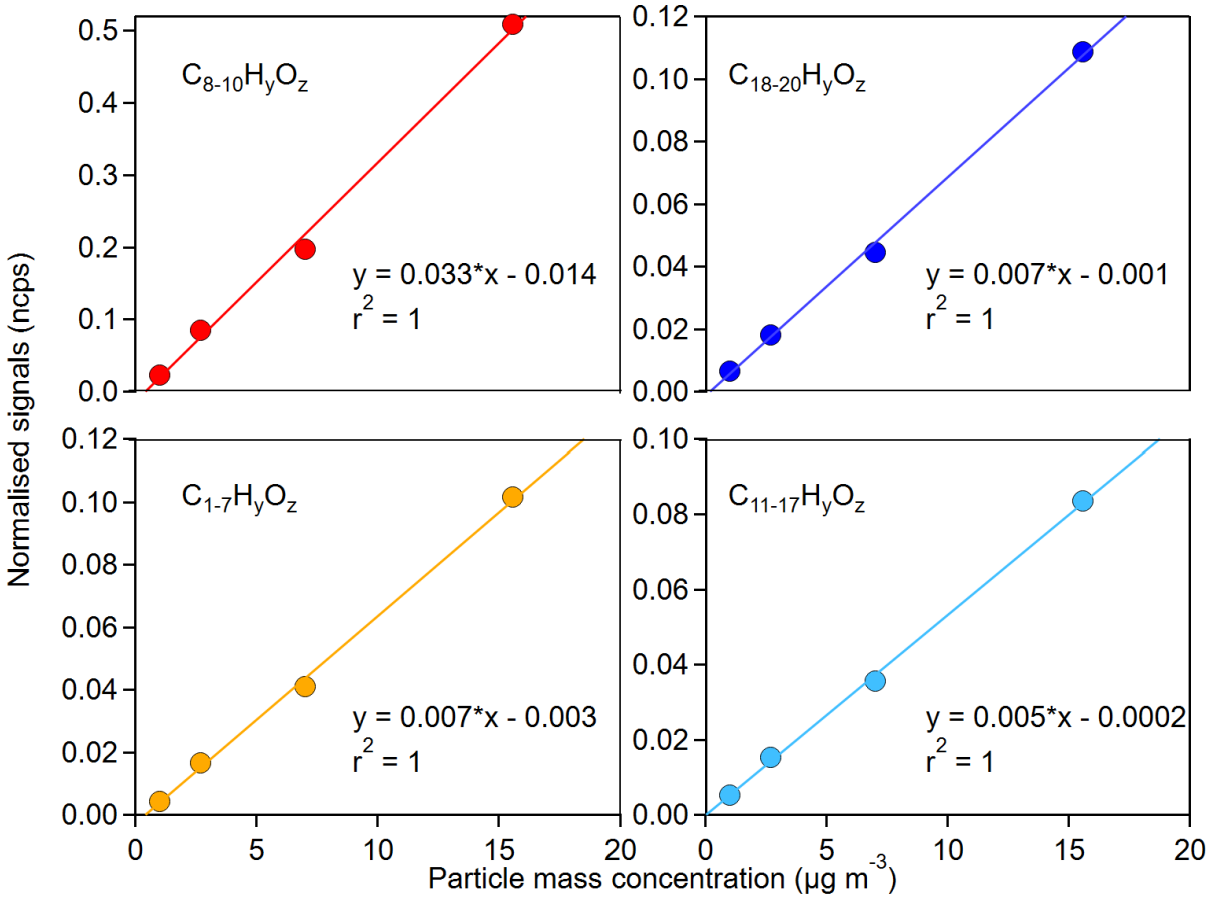

Figure S6. Measured signals of SOA α-pinene particle-phase compounds corresponding to the total aerosol mass concentrations.

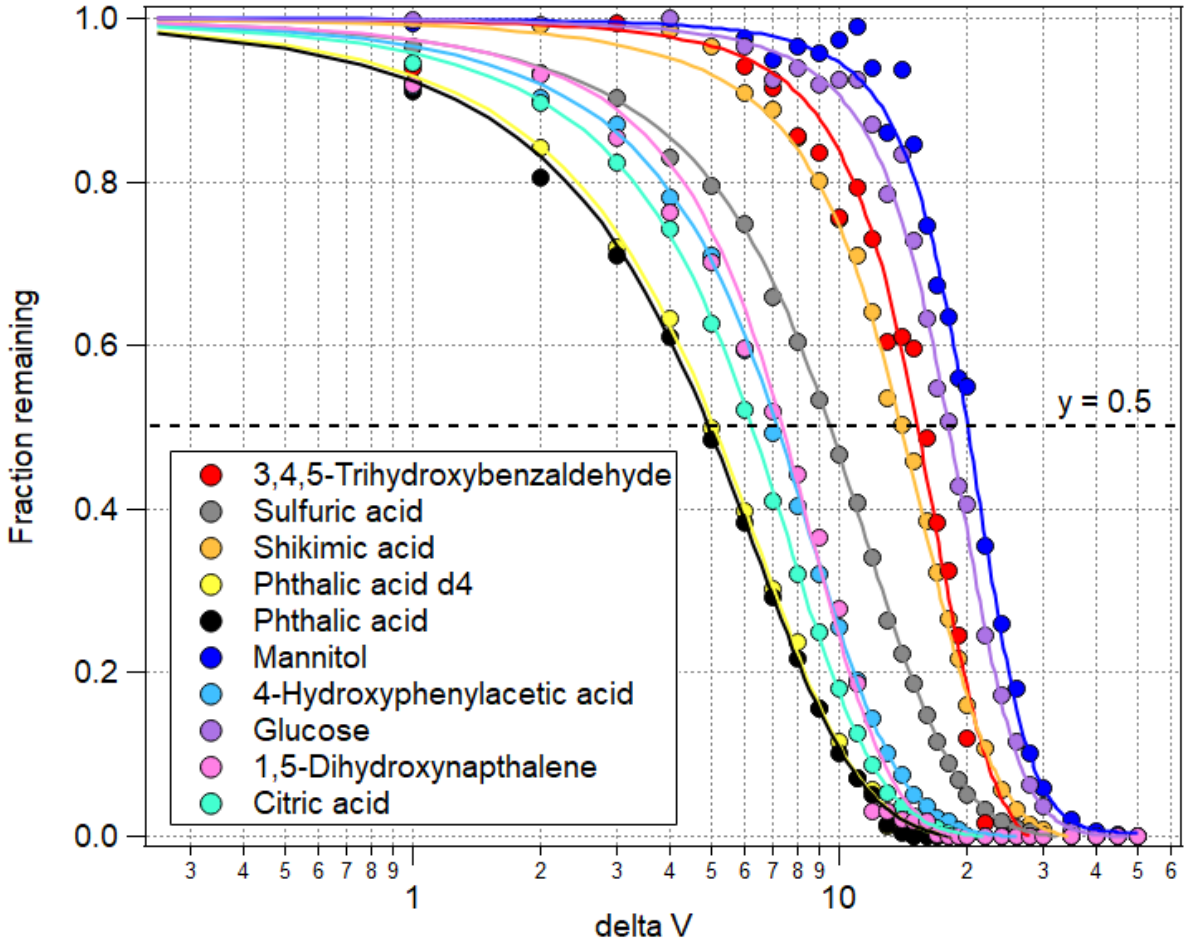

Figure S5. Declustering scans with increasing CID voltage and the remaining [M-Br]- intensity for each standard compound.

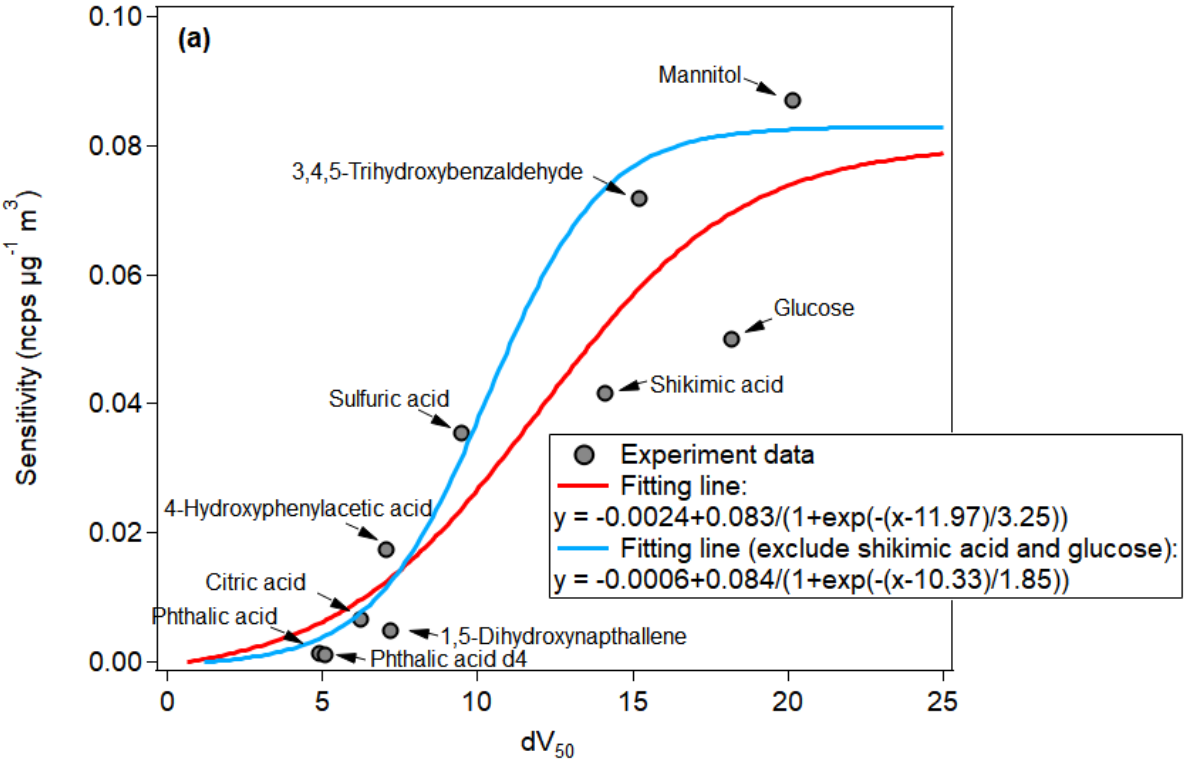

Figure S6. Correlation between sensitivity and the dV_{50} values for the standard chemicals.

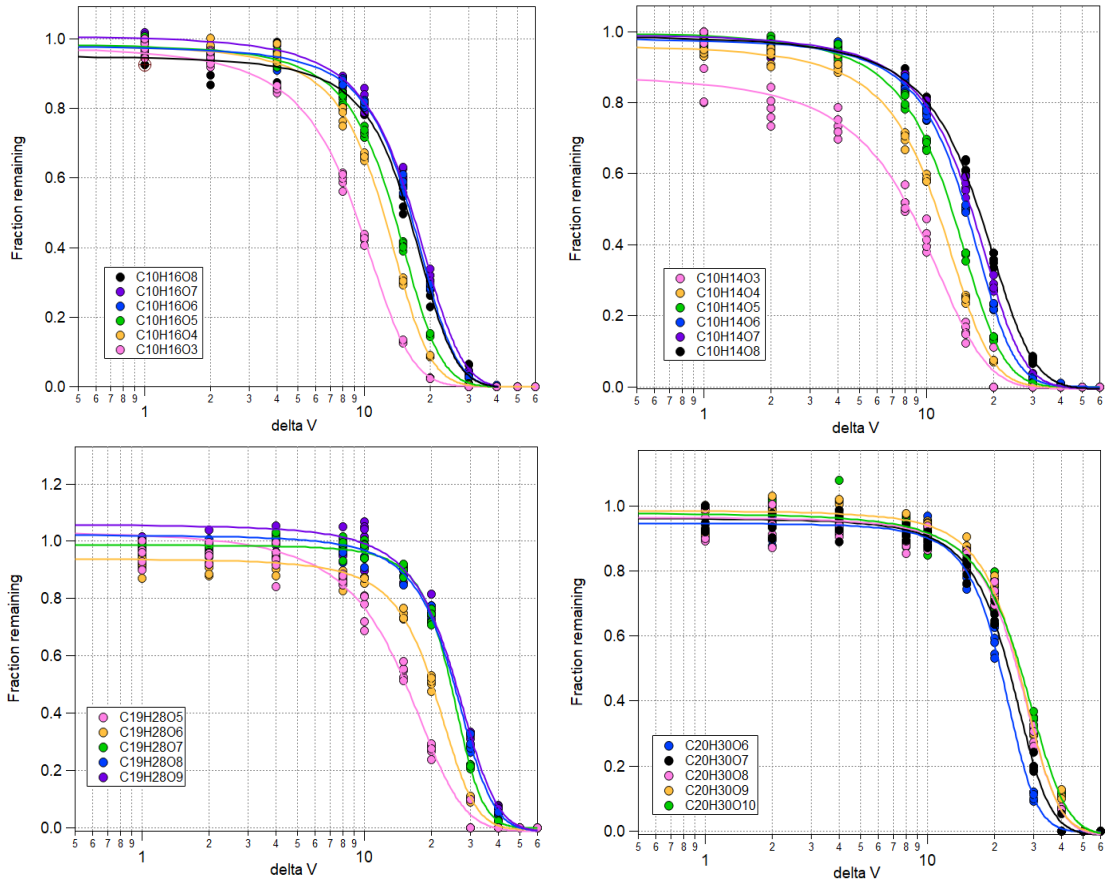

Figure S7. Declustering scans of C_{10} monomers and $C_{19\text{-}20}$ dimers measured from the OH/O_3 initiated oxidation α-pinene ozonolysis in the presence of SO_2 using the WALL-E CIMS.

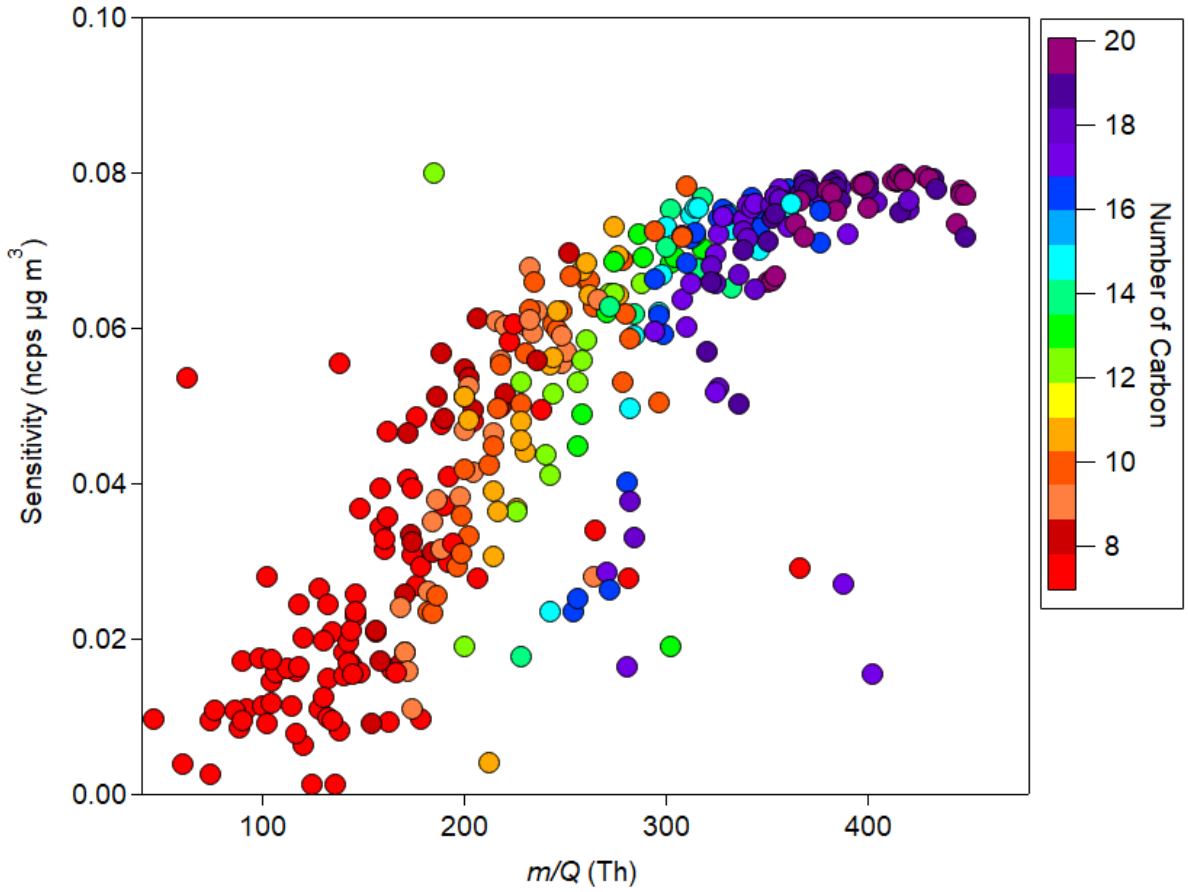

Figure S8. Sensitivity of SOA molecules based on their $dV_{50\ from}$ corresponding to their mass to charge ratios (m/Q).

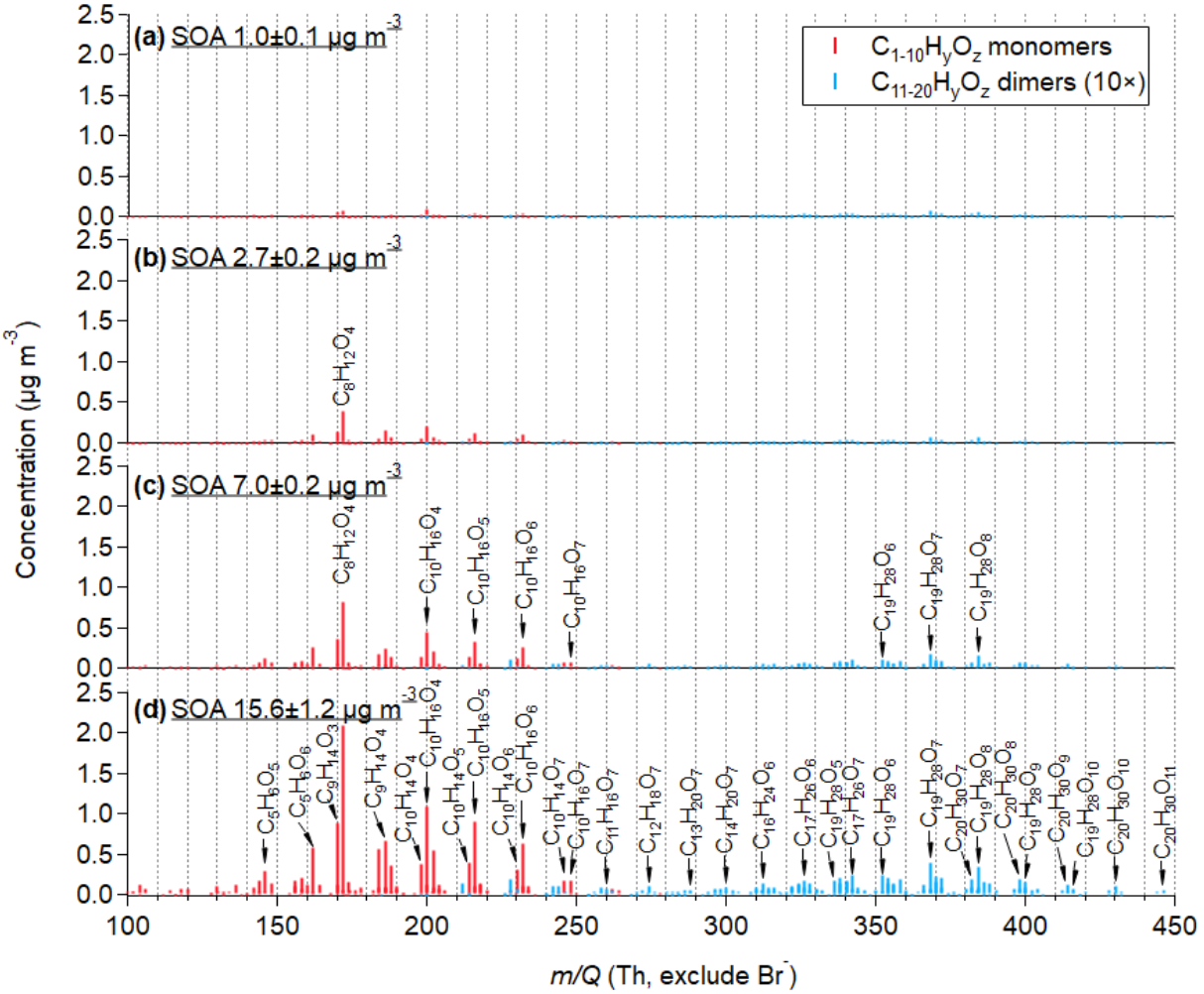

Figure S9. Quantified mass spectra in the mass concentration (μg m^{-3}) of SOA products corresponding to their mass to charge ratio (m/Q) under SOA concentrations between 1.0 ± 0.1 μg m^{-3} and 15.6 ± 1.2 μg m^{-3}. Red and blue sticks refer to monomers ($C_{1\text{-}10}H_yO_z$) and dimers ($C_{11\text{-}20}H_yO_z$), respectively. The identification of molecules is marked with black labels.

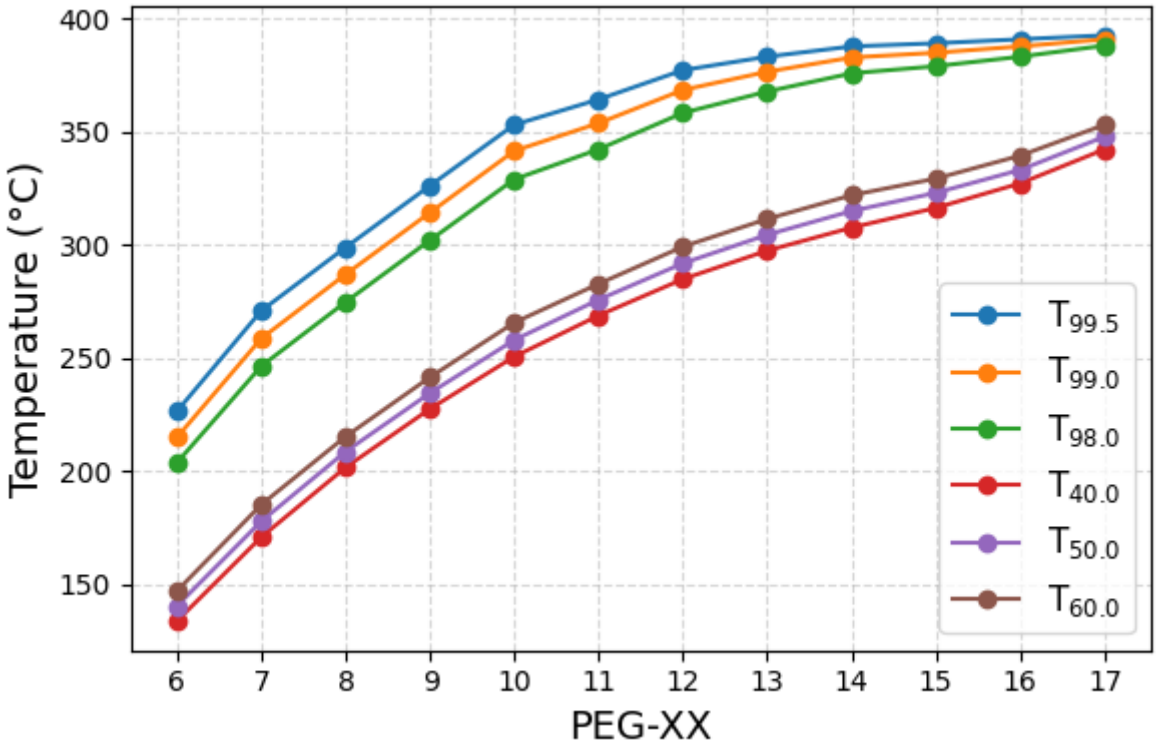

Figure S12. Effect of varying the signal percentage threshold on T_{max} determination in WALL-E PEG thermograms.

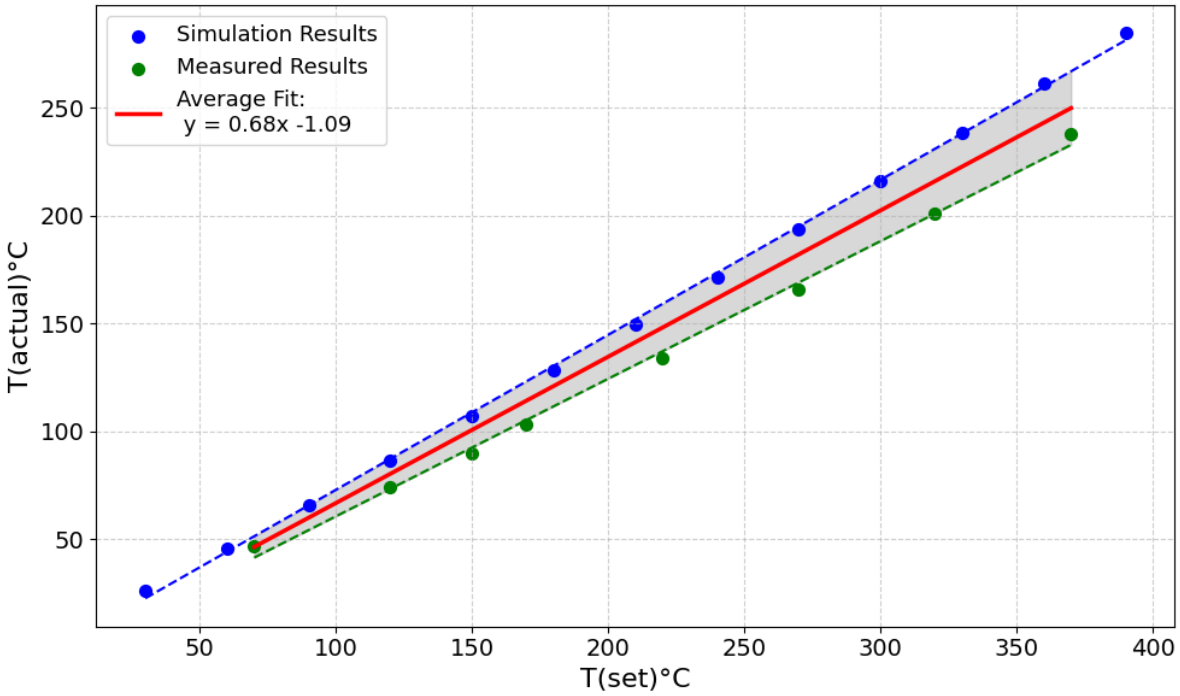

Figure S13. WALL-E temperature correction. T_{set} represents the set temperature for both hot sheath flow and TD and T_{actual} represents the simulated temperature.

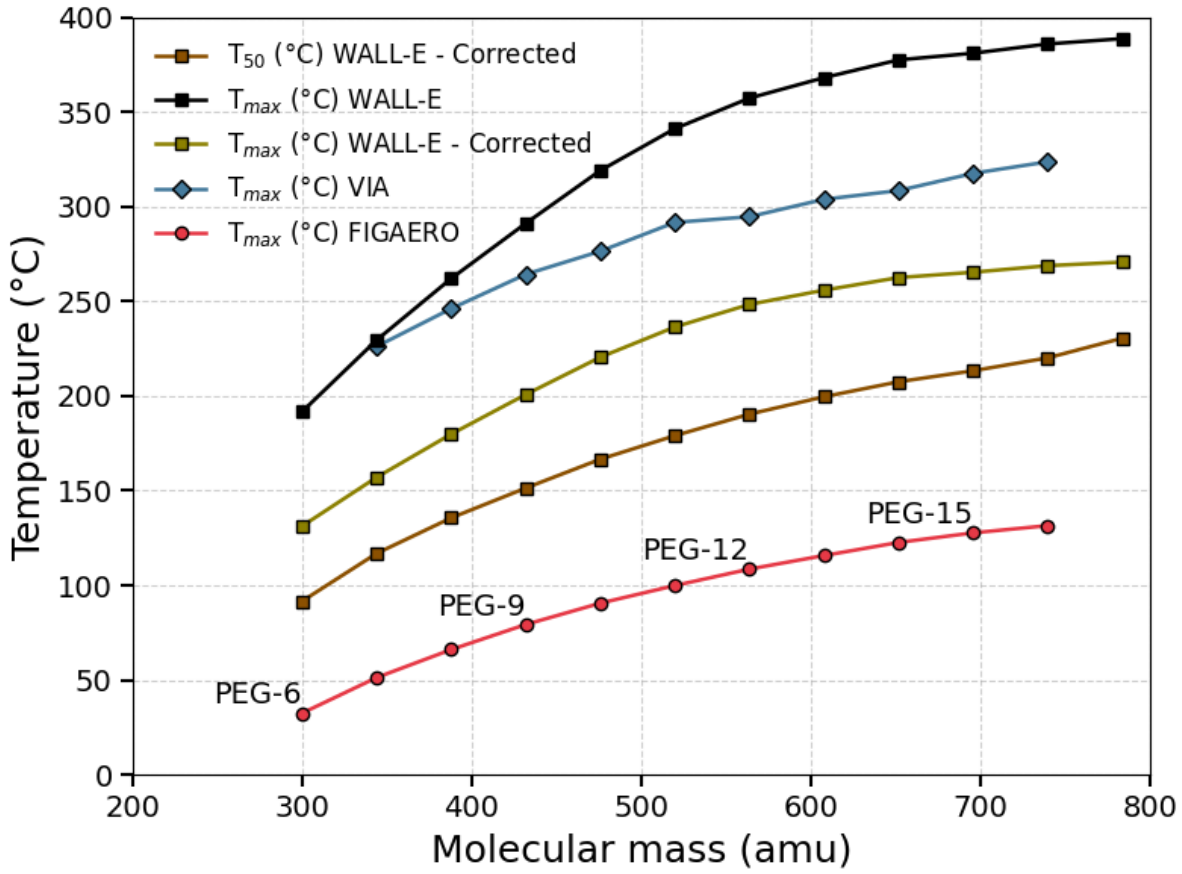

Figure S14. T_{max} and T_{50} as a function of molecular mass measured by WALL-E CIMS, VIA-CIMS and FIGAERO-CIMS (Zhao et al., 2024). WALL-E values are corrected using numerical simulations of gas flow to account for thermal lag and heat transfer dynamics in the thermal desorber.

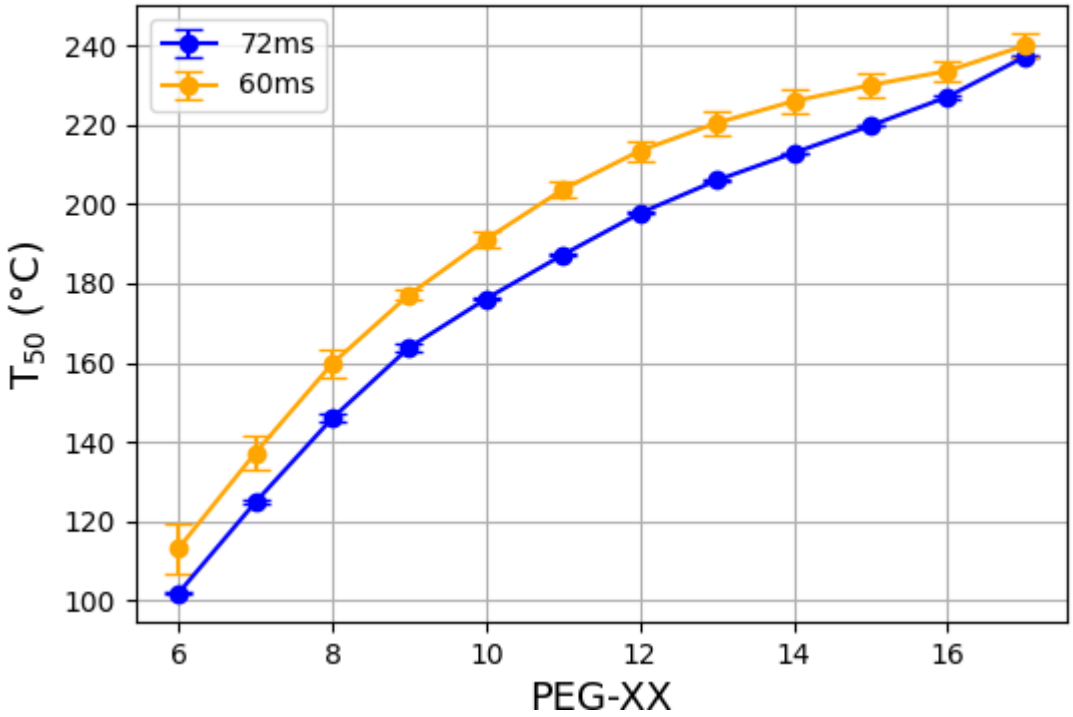

Figure S15. Effect of the residence time inside the TD region on the T_{max} corrected T_{50} values for PEG. 72ms represents a sample flow rate of 0.75 SLPM and HF of 0.25 SLPM, while 60ms represents SF of 1 SLPM and HF of 0.25 SLPM.

Table S1. Summary of conditions tested to characterize the optimal WALL-E setting parameters

Exp. No.	Sample flow (LPM)	Hot flow (LPM)	Hot sheath flow temp (°C)	TD temp (°C)
1	0.5	0	0	100
2	0.5	0	0	150
3	0.5	0	0	200
4	0.5	0	0	250
5	0.5	0	0	300
6	0.5	0	0	350
7	0.5	0.25	100	100
8	0.5	0.25	100	150
9	0.5	0.25	100	200
10	0.5	0.25	100	250
11	0.5	0.25	100	300
12	0.5	0.25	100	350
13	0.5	0.25	200	100
14	0.5	0.25	200	150
15	0.5	0.25	200	200
16	0.5	0.25	200	250
17	0.5	0.25	200	300
18	0.5	0.25	200	350
19	0.5	0.25	300	100
20	0.5	0.25	300	150
21	0.5	0.25	300	200
22	0.5	0.25	300	250
23	0.5	0.25	300	300
24	0.5	0.5	50	50
25	0.5	0.5	50	100
26	0.5	0.5	50	150
27	0.5	0.5	50	200
28	0.5	0.5	50	250
29	0.5	0.5	50	300
30	0.5	0.5	50	350
31	0.5	0.5	100	100
32	0.5	0.5	100	200
33	0.5	0.5	100	250
34	0.5	0.5	100	300
35	0.5	0.5	100	350
36	0.5	0.5	150	150
37	0.5	0.5	200	150
38	0.5	0.5	200	200
39	0.5	0.5	200	250
40	0.5	0.5	250	250
41	0.5	0.5	300	200
42	0.5	0.5	300	250
43	0.5	0.5	300	300
44	0.5	0.5	350	350
45	1	0	0	100
46	1	0	0	150

47	1	0	0	200
48	1	0	0	250
49	1	0	0	300
50	1	0	0	350
51	1	0.25	50	50
52	1	0.25	50	100
53	1	0.25	50	150
54	1	0.25	50	200
55	1	0.25	50	250
56	1	0.25	50	300
57	1	0.25	50	350
58	1	0.25	100	100
59	1	0.25	100	150
60	1	0.25	100	200
61	1	0.25	100	250
62	1	0.25	100	300
63	1	0.25	100	350
64	1	0.25	150	150
65	1	0.25	200	100
66	1	0.25	200	150
67	1	0.25	200	200
68	1	0.25	200	250
69	1	0.25	200	300
70	1	0.25	200	350
71	1	0.25	250	250
72	1	0.25	300	100
73	1	0.25	300	150
74	1	0.25	300	200
75	1	0.25	300	250
76	1	0.25	300	300
77	1	0.25	300	350
78	1	0.25	350	350
79	1	0.5	50	100
80	1	0.5	50	150
81	1	0.5	50	200
82	1	0.5	50	250
83	1	0.5	50	300
84	1	0.5	50	350
85	1	0.5	100	100
86	1	0.5	100	150
87	1	0.5	100	200
88	1	0.5	100	250
89	1	0.5	100	300
90	1	0.5	100	350
91	1	0.5	200	100
92	1	0.5	200	150
93	1	0.5	200	200
94	1	0.5	200	250
95	1	0.5	200	300
96	1	0.5	300	200

97	1	0.5	300	250
98	1	0.5	300	300
99	1	0.5	300	350
100	1.5	0	0	100
101	1.5	0	0	150
102	1.5	0	0	200
103	1.5	0	0	250
104	1.5	0	0	300
105	1.5	0	0	350
106	1.5	0.25	100	100
107	1.5	0.25	100	150
108	1.5	0.25	100	200
109	1.5	0.25	100	250
110	1.5	0.25	100	300
111	1.5	0.25	100	350
112	1.5	0.25	200	100
113	1.5	0.25	200	150
114	1.5	0.25	200	200
115	1.5	0.25	200	250
116	1.5	0.25	200	300
117	1.5	0.25	200	350
118	1.5	0.25	300	100
119	1.5	0.25	300	150
120	1.5	0.25	300	200
121	1.5	0.25	300	250
122	1.5	0.25	300	300
123	1.5	0.25	300	350
124	1.5	0.5	50	50
125	1.5	0.5	50	100
126	1.5	0.5	50	150
127	1.5	0.5	50	200
128	1.5	0.5	50	250
129	1.5	0.5	50	300
130	1.5	0.5	50	350
131	1.5	0.5	100	100
132	1.5	0.5	100	150
133	1.5	0.5	100	200
134	1.5	0.5	100	250
135	1.5	0.5	150	150
136	1.5	0.5	200	200
137	1.5	0.5	Signal decrease	250
138	1.5	0.5	200	300
139	1.5	0.5	200	350
140	1.5	0.5	250	250
141	1.5	0.5	300	100
142	1.5	0.5	300	200
143	1.5	0.5	300	250
144	1.5	0.5	300	300
145	1.5	0.5	350	350

Table S2. Sensitivity of standard compounds.

Compounds	Concentrations of aqueous solution (ppm)	Slope (Sensitivity, ncps per μg m^{-3})	Density used for SMPS (g/m^3)	R-square of fitting
3,4,5-trihydroxybenzaldenhyde	1	0.0718 ± 0.0033	1.37	0.94
sulfuric acid	1	0.0263 ± 0.0011	1.77*	0.95
shikimic acid	1	0.0417 ± 0.0022	1.52	0.93
phthalic acid d4	1	0.0011 ± 0.0000	1.59	0.99
phthalic acid	1	0.0013 ± 0.0001	1.59	0.96
mannitol	2	0.0870 ± 0.0020	1.52	0.99
4-hydroxyphenylacetic acid	1	0.0174 ± 0.0006	1.21	0.97
glucose	1	0.0499 ± 0.0013	1.56	0.98
1,5-dihydroxynapthalene	NA	0.0050 ± 0.0004	1.09	0.85
citric acid	1	0.0066 ± 0.0002	1.54	0.95

*1.77g/m^3 is the density of Ammonium Sulfate.

Table S3. Summary of conditions of SOA experiments

Exp. No.	α-pinene (ppb)	SO_2 (ppb)	Relative humidity	Particle mass (µg m-3)
0	0	31	dry	0
1	11	31	dry	0.8±0.1
2	28	31	dry	2.2±0.2
3	56	31	dry	5.8±0.2
4	112	31	dry	12.9±1

Table S4. Summary of conditions of PEG experiments

Compound	T_{max} (uncorrected)	T_{max} Corrected	Fragmentation ratio at 390°C
PEG-6	203.6	143.7	11.2
PEG-7	246.3	172.8	18.9
PEG-8	274.6	192.1	16.7
PEG-9	301.9	210.7	12.8
PEG-10	328.8	229.1	9
PEG-11	342.1	238.2	6
PEG-12	358.2	249.1	7.4
PEG-13	367.6	255.6	5.5
PEG-14	375.7	261.1	3.7
PEG-15	378.8	263.2	2.3
PEG-16	383	266.1	2.3
PEG-17	387.9	269.4	-2.4

Reference

Zhao, J., Mickwitz, V., Luo, Y., Häkkinen, E., Graeffe, F., Zhang, J., Timonen, H., Canagaratna, M., Krechmer, J. E., Zhang, Q., Kulmala, M., Kangasluoma, J., Worsnop, D., and Ehn, M.: Characterization of the Vaporization Inlet for Aerosols (VIA) for online measurements of particulate highly oxygenated organic molecules (HOMs), Atmos. Meas. Tech., 17, 1527-1543, 10.5194/amt-17-1527-2024, 2024.